Supporting Information

A Polarized Luminescent Thermometer based on Dye Encapsulated Metal-Organic Framework

Shenghan Lin [a, ⊥], Zhengluan Liao [a, ⊥], Heqi Zheng [a], Chenyu Li [a], Yuanjing Cui [a, b] *, Zhiyu Wang [a], Guodong Qian [a, *]

[a] *State Key Laboratory of Silicon and Advanced Semiconductor Materials, School of Materials Science & Engineering, Zhejiang University, Hangzhou 310027, China.*

[b] *ZJU-Hangzhou Global Scientific and Technological Innovation Center, Zhejiang University, Hangzhou 311215, China.*

E-mail: cuiyj@zju.edu.cn, gdqian@zju.edu.cn

1. Experimental section

Material characterization

Powder X-ray diffraction (PXRD) patterns were collected on an X'Pert PRO diffractometer with Cu Kα radiation (λ = 1.542 Å) at room temperature, in the range of 2θ = 5-45º. UV-vis absorption spectroscopy was measured with UV-2600 UV-vis spectrophotometer (Shimadzu, Japan). The one-photon excited fluorescence spectra were obtained on a Hitachi F-4600 fluorescence spectrometer at room temperature. Thermogravimetric analyses (TGA) were obtained on a Netzsch TG209F3 under N_2 atmosphere with a heating rate of 10 K min^{-1}, the testing temperature was set from 30 ℃ to 800 ℃. The microscopy images of crystals were captured on an Olympus IX 71 inverted fluorescent microscope under the irradiation of halogen lamps and mercury lamps The corresponding emission spectra were recorded by the fiber optic spectrometer (PG2000-Pro, Ideaoptics Instruments). Fourier transform infrared (FTIR) spectra were recorded on a Thermo Fisher Nicolet iS10 spectrometer by using KBr pallets. The pallets were fabricated by mixing the sample and KBr. The mixture was then grinded and compressed under a pressure of 400 kgf cm^{-2} to form the transparent pallets. The solid samples were added into $BaSO_4$ before tests. The quantum yield was recorded on an Edinburgh Instrument F920 spectrometer. The ^1H nuclear magnetic resonance (NMR) spectrum was obtained from a Bruker Advance DMX500 spectrometer. The ZJU-28 ⊃DSM (10 mg) was dissolved in DMSO-d_6 with 20 μL DCl.

Polarization emission spectra test.

The sample were put on the microscope stage in Fig. S14. One isolated crystal was chosen to be excited by a polarized fs laser (532 nm). During the test, the sample and stage were not moved and touched at all. A half wave plate was rotated to change the polarized direction of the incident laser, and the corresponding signals were recorded by a high-resolution fiber optic spectrometer (PG2000-Pro, Ideaoptics Instruments).

Temperature detection

The temperature is controlled by water bath circulation, (and the detection temperature range is 293-305 K and 293-313 K). Fix the powder in the groove of the copper plate and stick it on the temperature-controlled pipe of the water bath. The temperature of the water bath is first set to a minimum temperature of 293 K, and then the temperature is gradually increased, and a point is

tested at an interval of 2 K and 5 K, and the test starts after the temperature is stable for 30 minutes at each temperature point.

2. Supplementary Figures

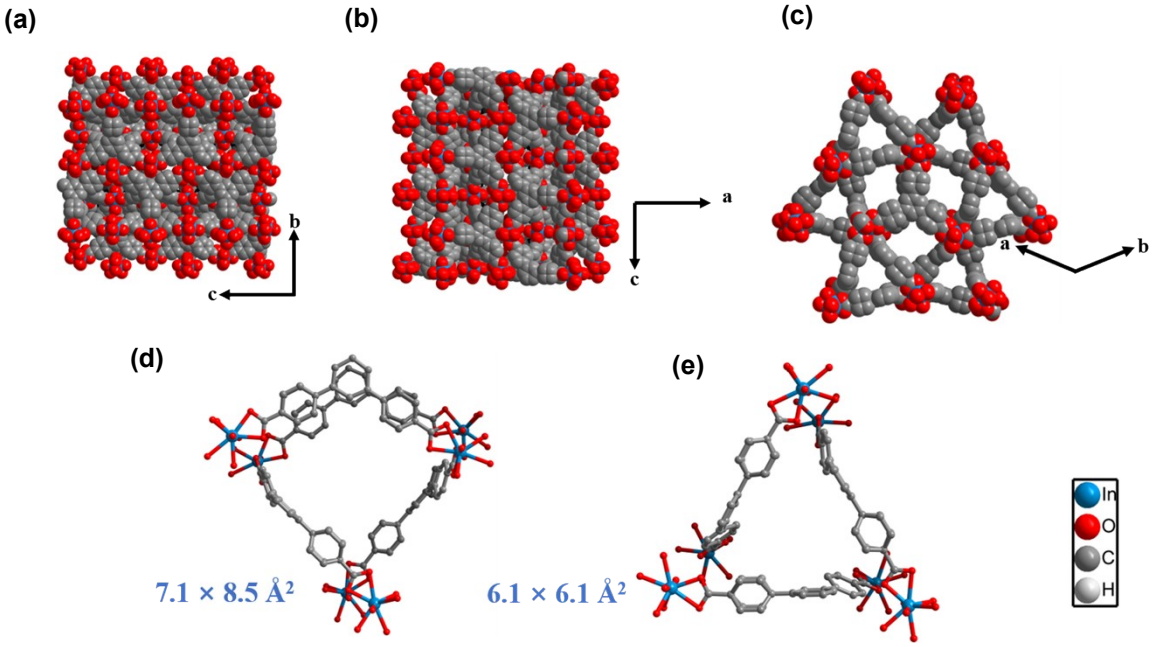

Fig. S1. The Space filling model structure of ZJU-28- along (a) *a*-axis, (b) *b*-axis, and (c)*c*-axis, which show 1D channels along *c*-axis. The 1D channels have two different pore sizes of (d) 6.1 × 6.1 Å^2 and (e) 7.1 × 8.5 Å^2.

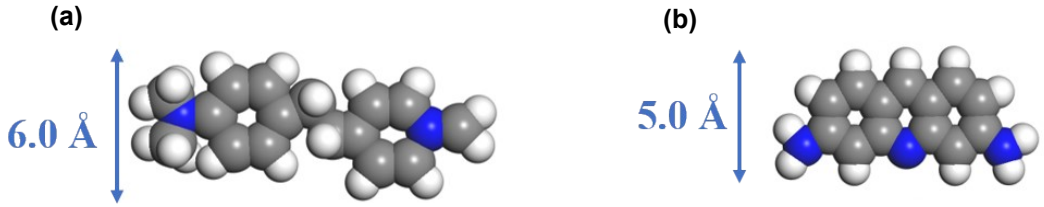

Fig. S2. The Space filling model of (a) DSM and (b) ACF.

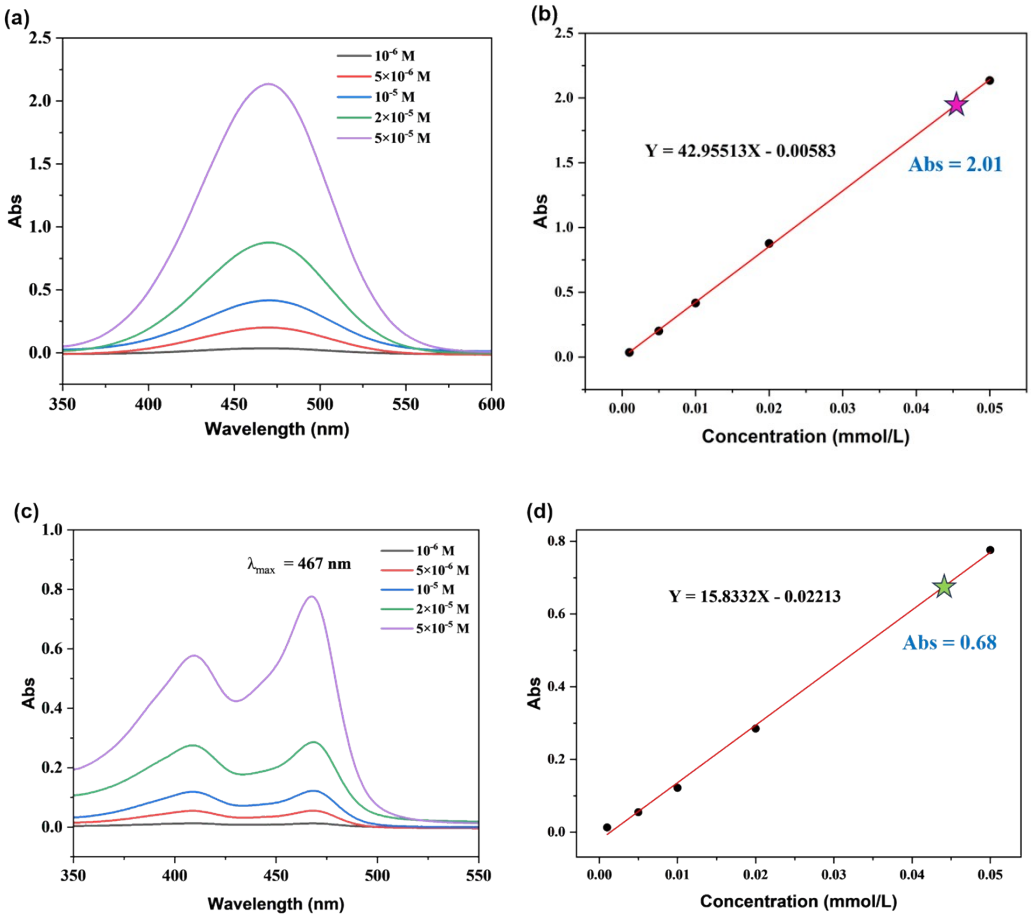

Fig. S3. (a) and (c) The absorbance-concentration diagram and the fitted curve for the DSM and ACF solution in DMF. (b) and (d) The linear relationship between DSM contents and absorbance peaks (λ_{max} = 470 nm). The DSM and ACF concentration in the obtained **ZJU-28⊃DSM** and **ZJU-28⊃ACF** composites was determined to be about 29.08 wt% and 21.05 wt%.

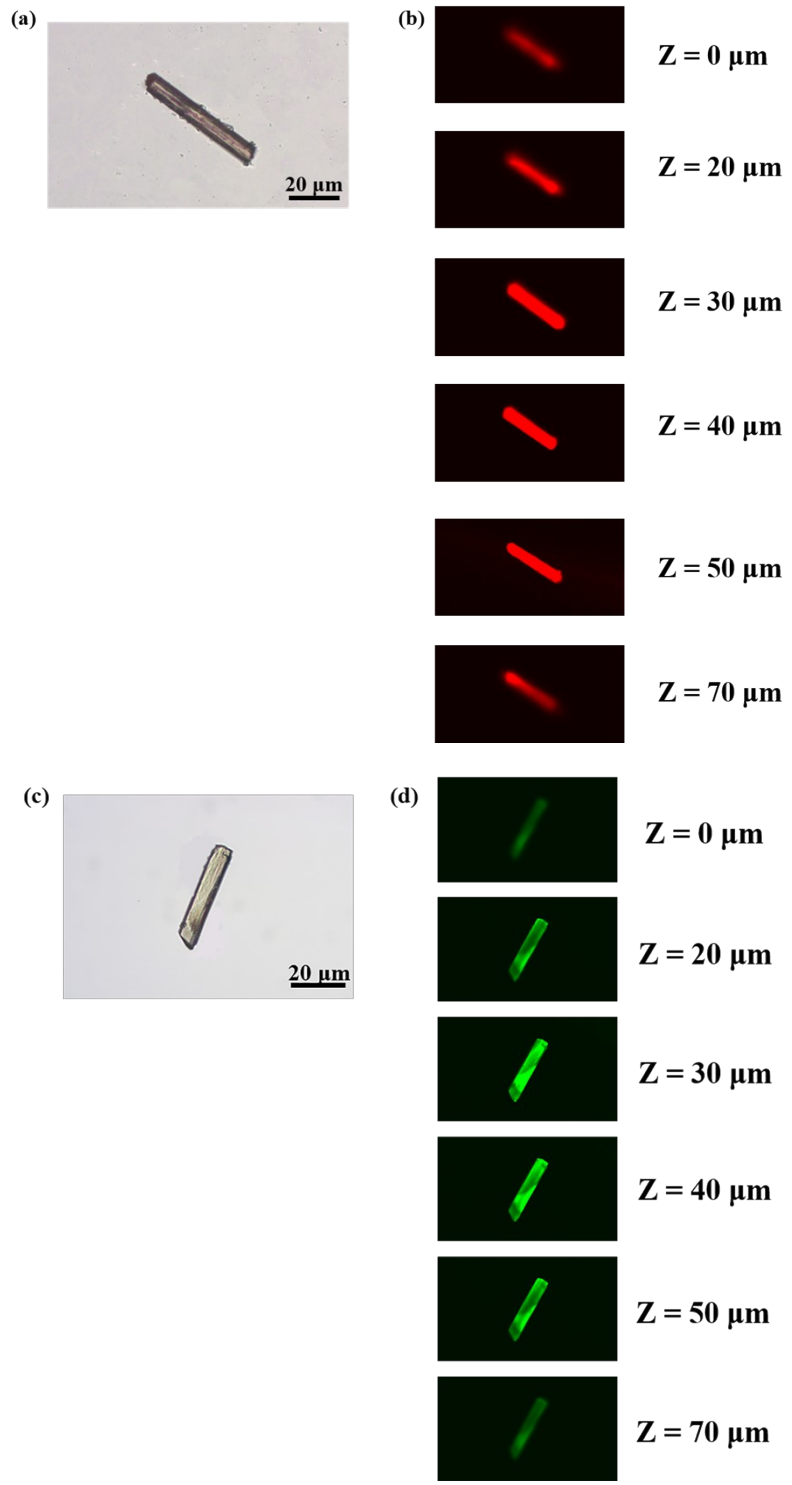

Fig. S4. (a) Optical microscopy image of **ZJU-28⊃DSM** single crystal under natural light. Scale bar: 20 μm. (b) Fluorescent confocal images of **ZJU-28⊃DSM** single crystal at different depths. Excitation wavelength: 558 nm. (c) Optical microscopy image of **ZJU-28⊃ACF** single crystal under natural light. Scale bar: 20 μm. (d) Fluorescent confocal images of **ZJU-28⊃ ACF** single crystal at different depths. Excitation wavelength: 488 nm.

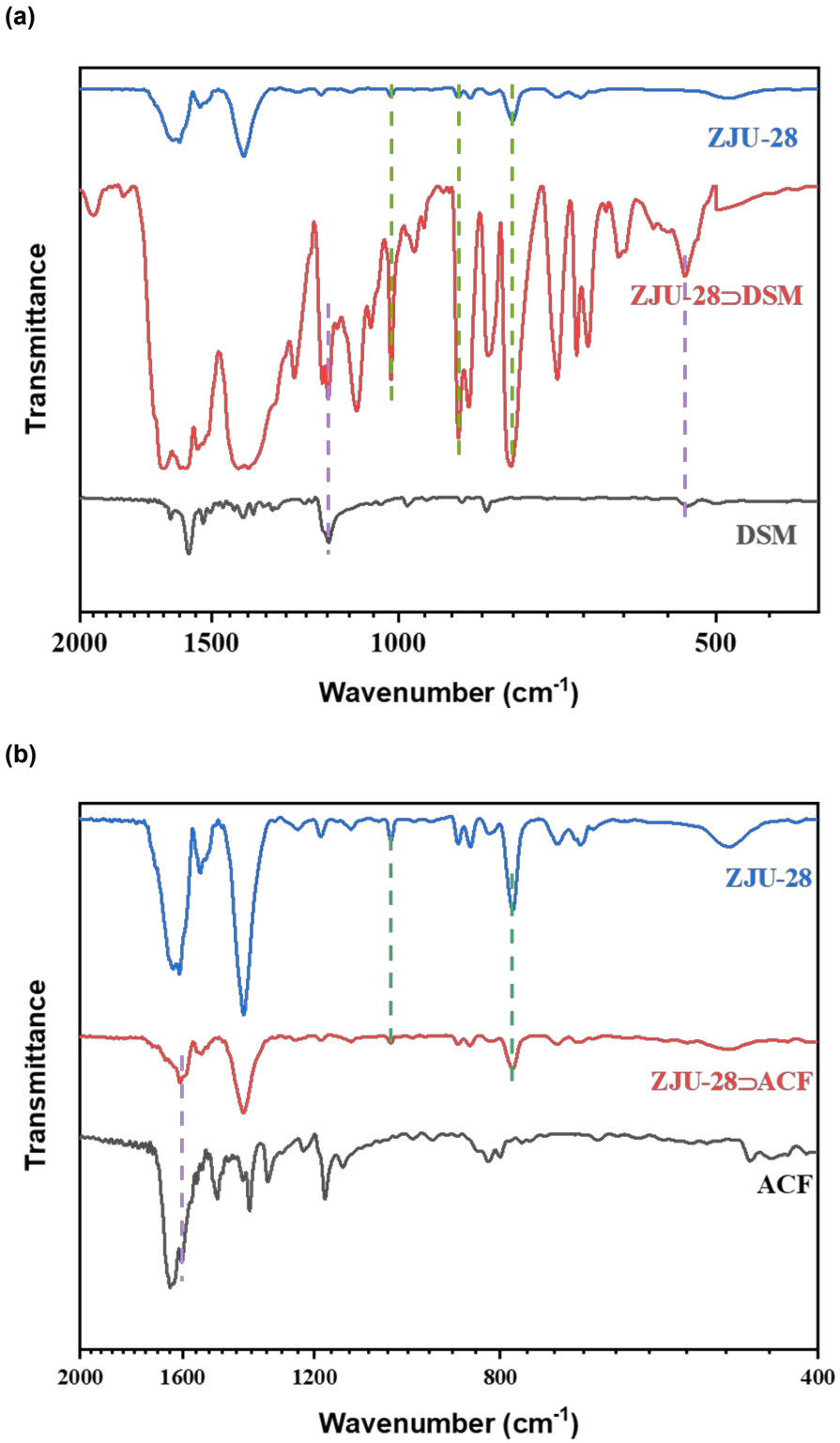

Fig. S5. (a) FTIR spectra of ZJU-28, ZJU-28⊃DSM and DSM. (b) FTIR spectra of ZJU-28, ZJU-28⊃ACF and ACF.

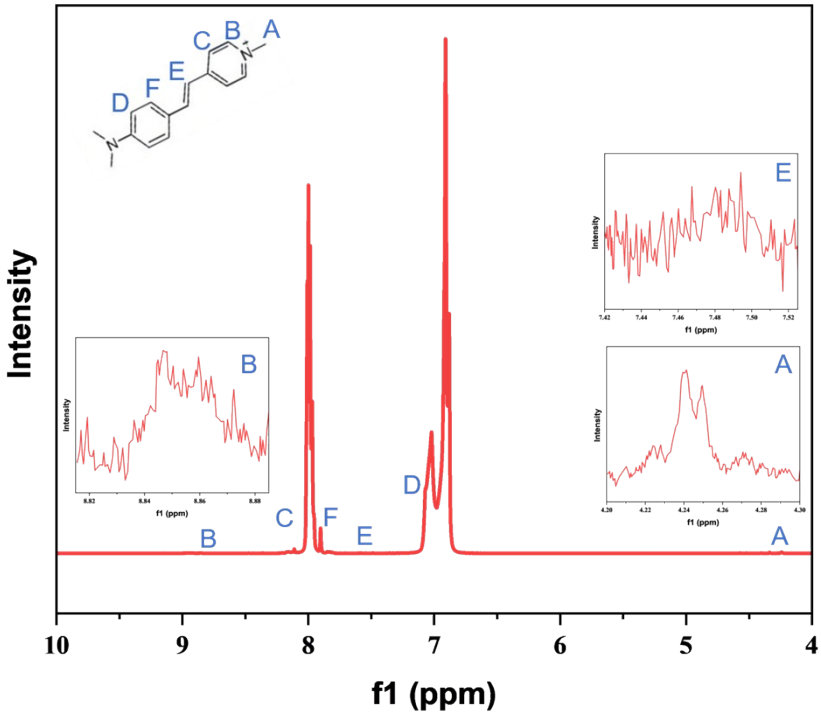

Fig. S6. The ^{1}H NMR (500MHz) spectrum of ZJU-28⊃DSM dissolved in DMSO-d_6 and DCl. Inset: the amplified NMR spectrum of ZJU-28⊃DSM in the corresponding range.

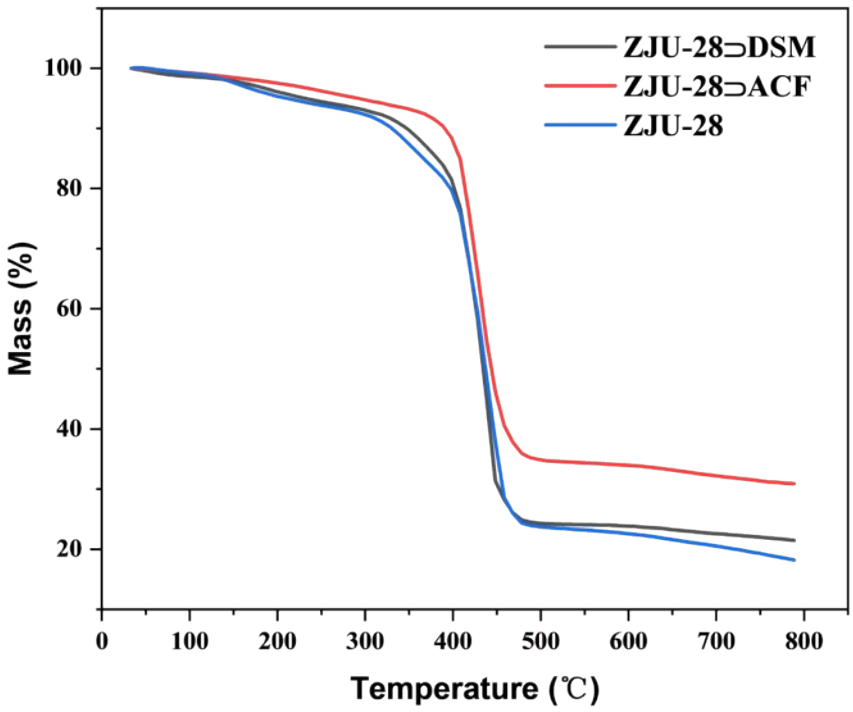

Fig S7. The TGA curve of ZJU-28, ZJU-28⊃DSM and ZJU-28⊃ACF.

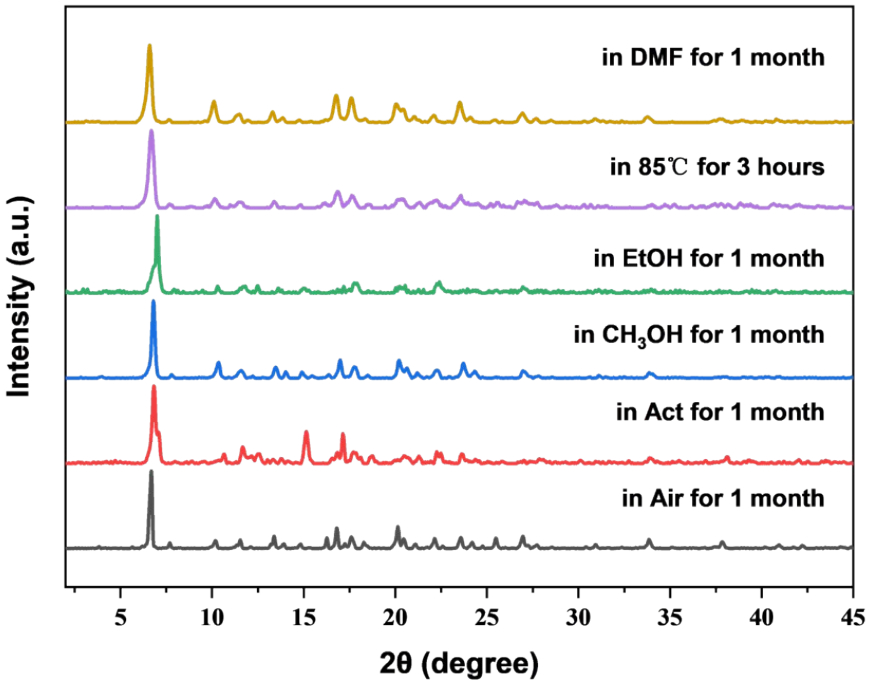

Fig. S8. PXRD patterns of ZJU-28⊃DSM in the air and common solvents such as acetone, ethanol, methanol and DMF, and after heat treatment, showing good chemical stability.

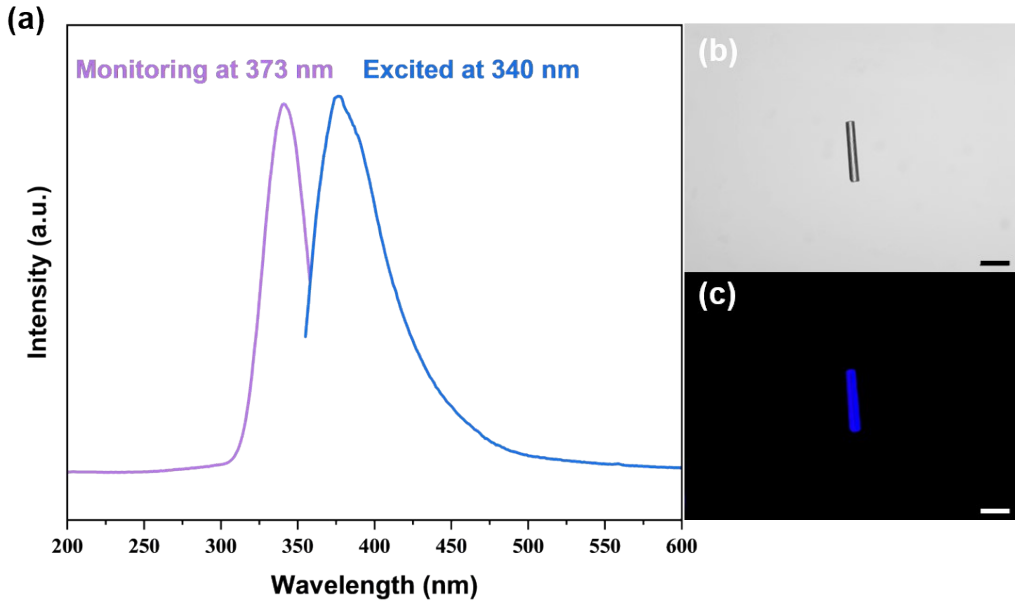

Fig S9. Excitation and emission spectra of ZJU-28 crystals. The microscopy images of an isolated ZJU-28 microcrystal under (b) day light and (c) UV light.

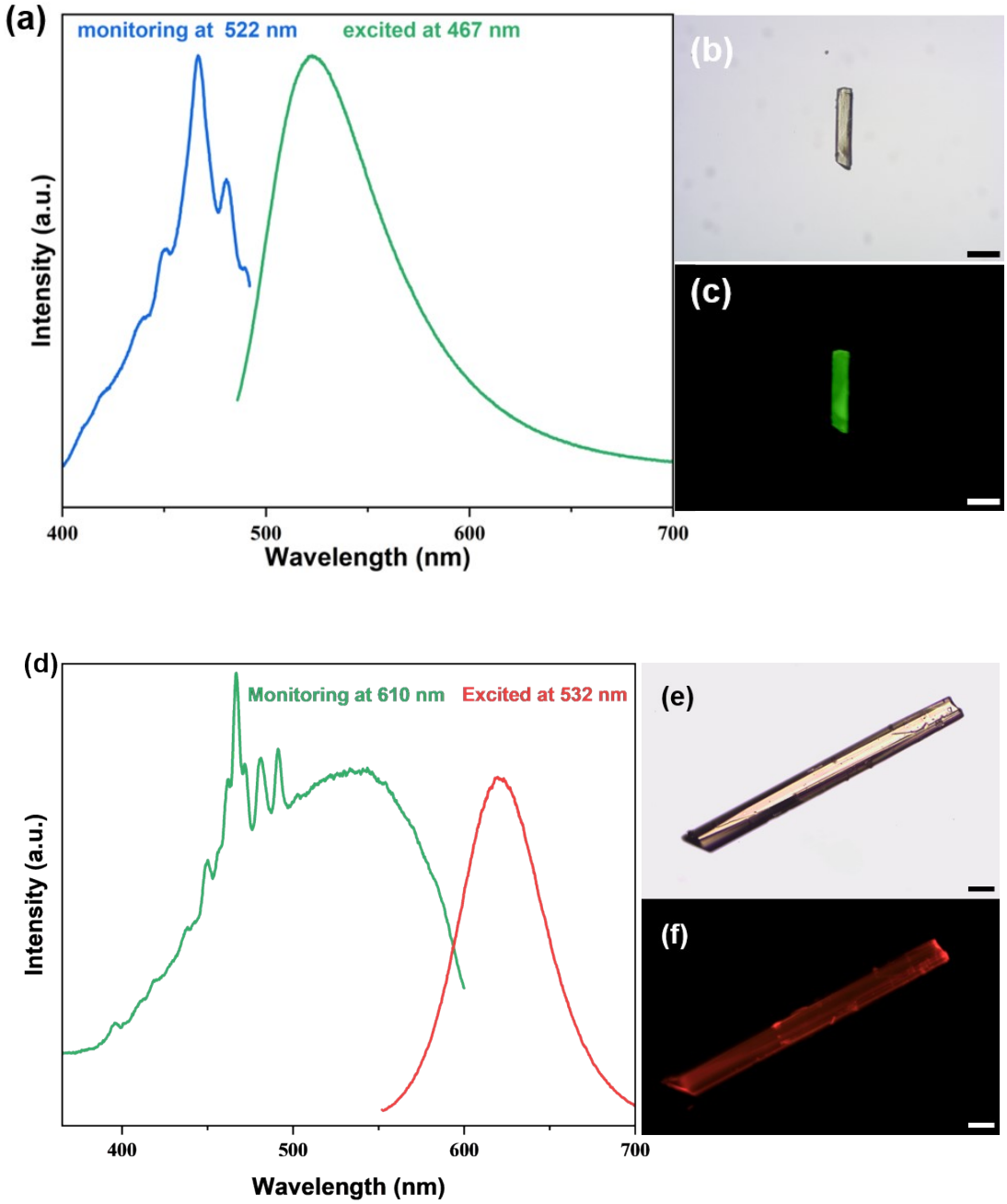

Fig S10. Excitation and emission spectra of **ZJU-28⊃ACF** crystals. The microscopy images of an isolated **ZJU-28⊃ACF** microcrystal under (b) day light and (c) UV light. (d) Excitation and emission spectra of **ZJU-28⊃DSM** crystals. The microscopy images of an isolated **ZJU-28⊃DSM** microcrystal under (e) day light and (f) UV light. Scale bar, 50 μm

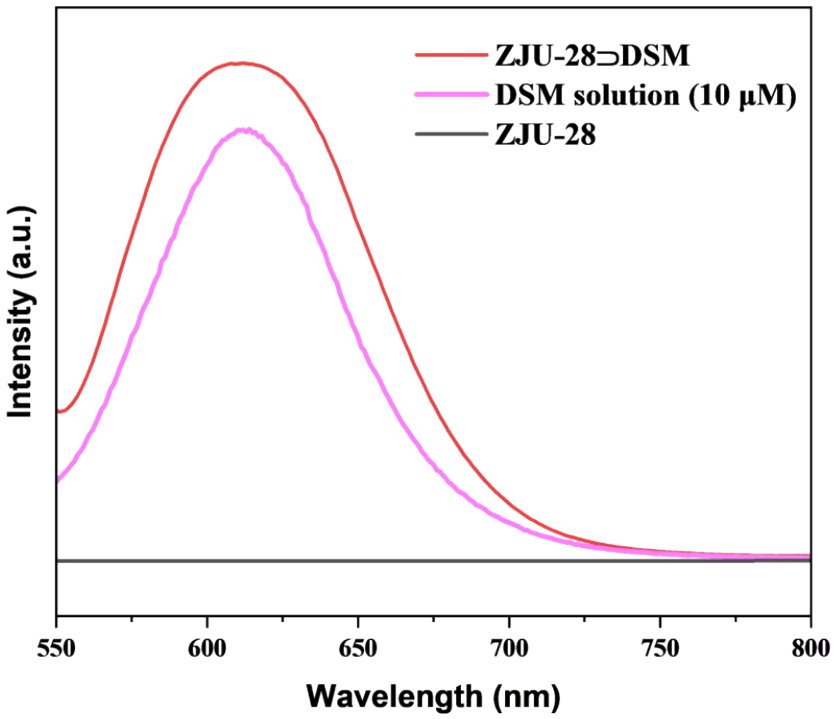

Fig. S11. Emission Spectra (λ_{Ex} = 532 nm) of DSM solution (10 μM), ZJU-28 and ZJU-28⊃DSM.

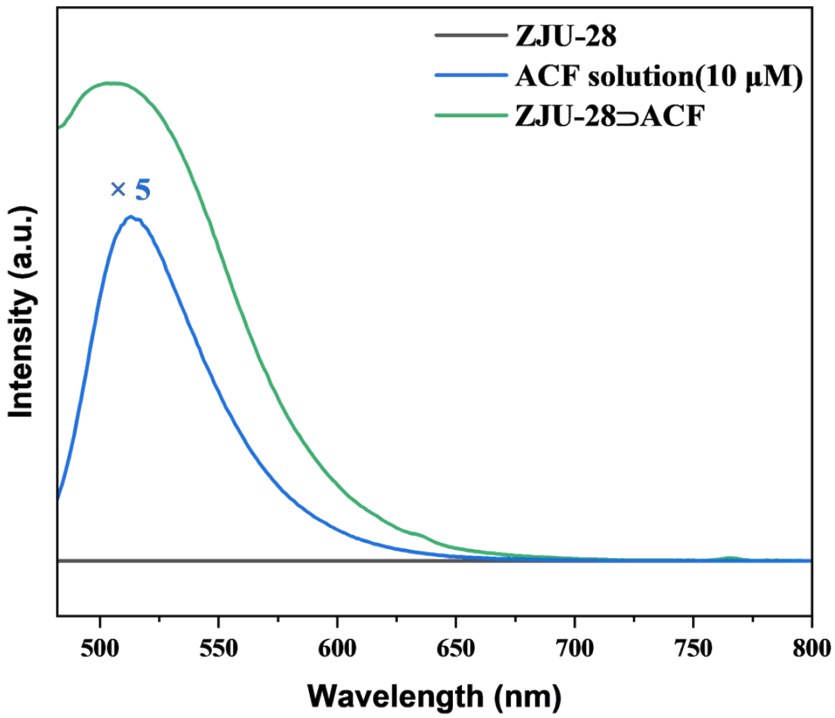

Fig. S12. Emission Spectra (λ_{Ex} = 467 nm) of ACF solution (10 μM), ZJU-28 and ZJU-28⊃ACF.

Table S1. Photoluminescence Quantum yields of ZJU-28, ZJU-28⊃DSM and DSM solution, excited at 532 nm.

Sample	Photoluminescence Quantum Yields [%]
ZJU-28	0
ZJU-28⊃DSM (21.05 wt% ACF)	27.41
DSM solution (10 uM)	0.14

Table S2. Photoluminescence Quantum yields of ZJU-28, ZJU-28⊃ACF and ACF solution, excited at 467 nm.

Sample	Photoluminescence Quantum Yields [%]
ZJU-28	0
ZJU-28⊃ACF (21.05 wt% ACF)	27.35
ACF solution (10 uM)	20.11

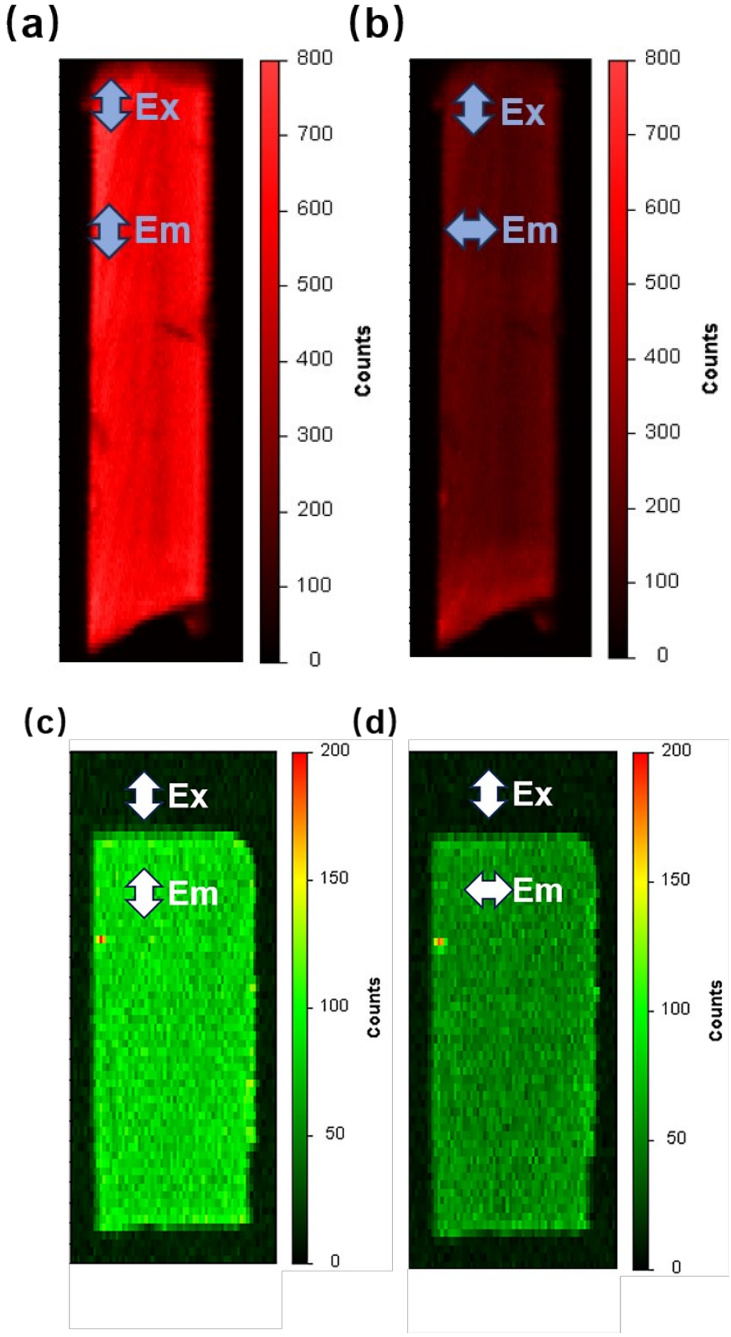

Fig. S13. Polarization fluorescence images of a single **ZJU-28⊃DSM** crystal when the emission polarization direction is (a) parallel or (b) perpendicular to the crystal longitudinal direction and a single **ZJU-28⊃ACF** crystal when the emission polarization direction is (c) parallel or (d) perpendicular to the crystal longitudinal direction.

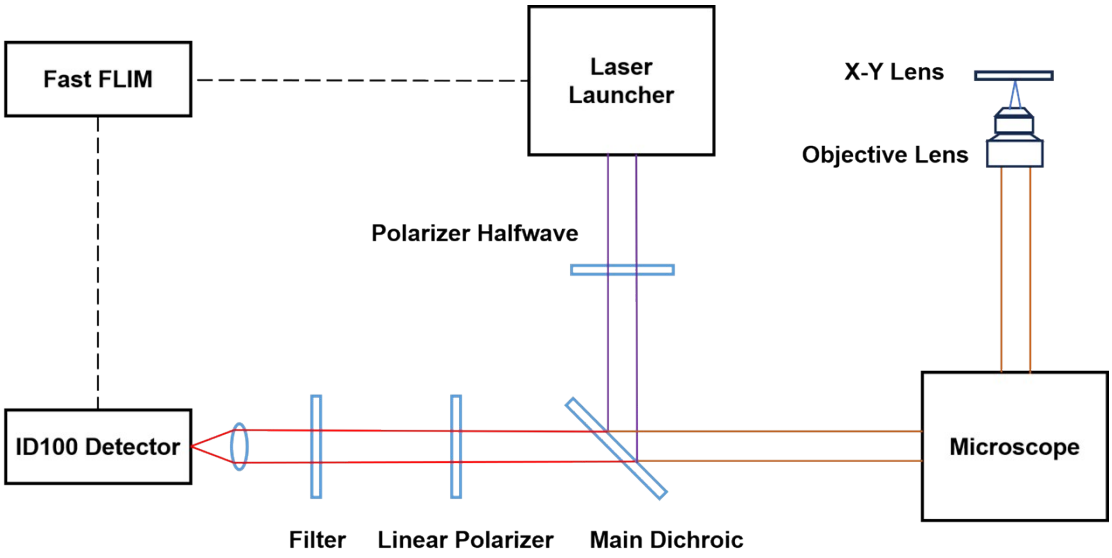

Fig. S14. Schematic diagram of the experimental device for polarization fluorescence imaging conducted by recording the number of photons. The excitation polarization direction is kept parallel with the longitudinal direction of **ZJU-28⊃DSM** and **ZJU-28⊃ACF** crystals, and a linear polarizer is set before the single photon counting detector ID-100 to control the received photon numbers from the excited crystal. On account of the poor fluorescence of ZJU-28, almost all the photon numbers from the **ZJU-28⊃DSM** and **ZJU-28⊃ACF** crystals were thought to come from DSM and ACF molecules. The Fast FLIM module can be employed to record the lifetime of the sample.

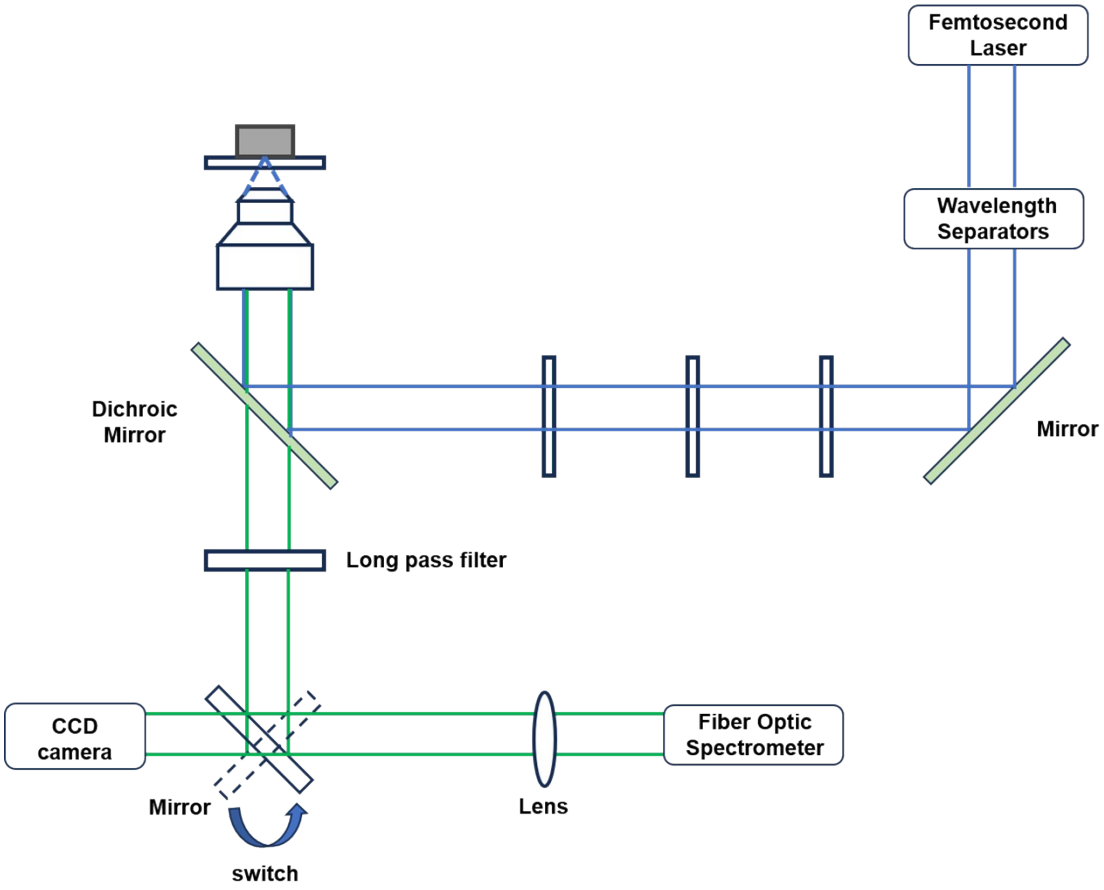

Fig. S15. Experimental setup for measuring emission signals of a single crystal with different excitation polarization direction. The polarizer is used to purify the pump laser source. The polarization direction of the excitation light by rotating the half-wave plate, which is kept either parallel or perpendicular to the longitudinal direction of crystal. The half-wave plate is only used for the excitation polarization dependence measurements, and it can be dismounted when the tests are unrelated to polarization measurements. Detect include the CCD camera and fiber optic spectrometer.

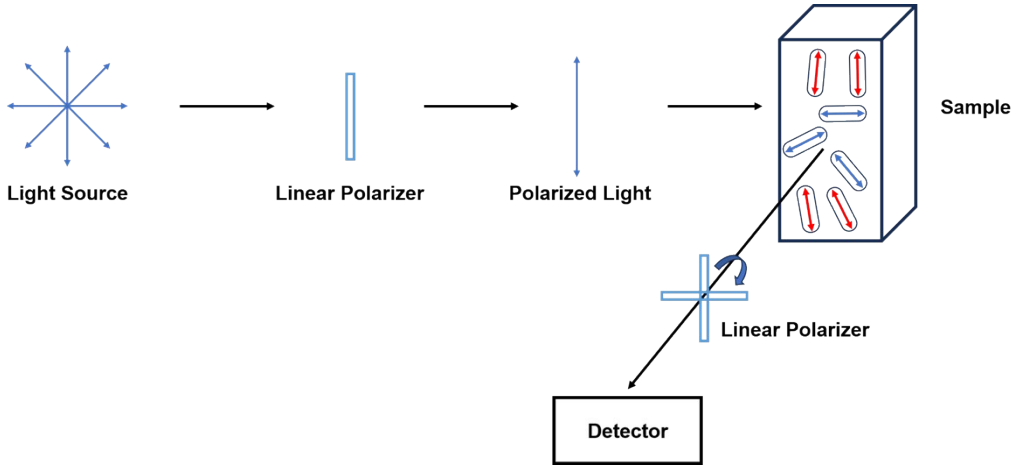

Fig. S16. Schematic diagram of the experimental device for polarization fluorescence of temperature response conducted by recording the fluorescence intensity. Light first passes through a linear polarizer to become linearly polarized light, which is then projected onto the surface of the powder platform equipped with a temperature control device. The emitted light once again passes through a linear polarizer and is received by a sensor.

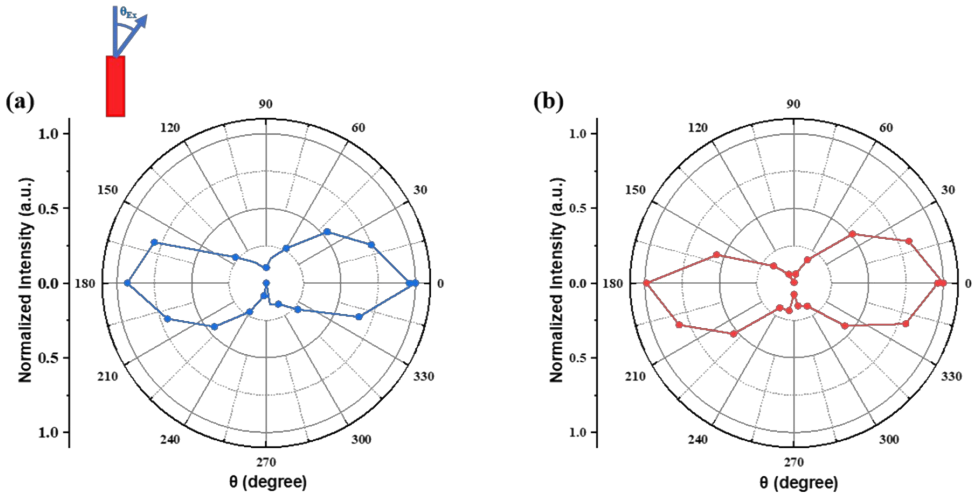

Fig. S17. Polar plots of a **ZJU-28⊃DSM** crystal at (a) 297 K and (b) 309 K as the function of θ_{Ex}. Inset: the schematic illustration of the measurement geometry for a single crystal.

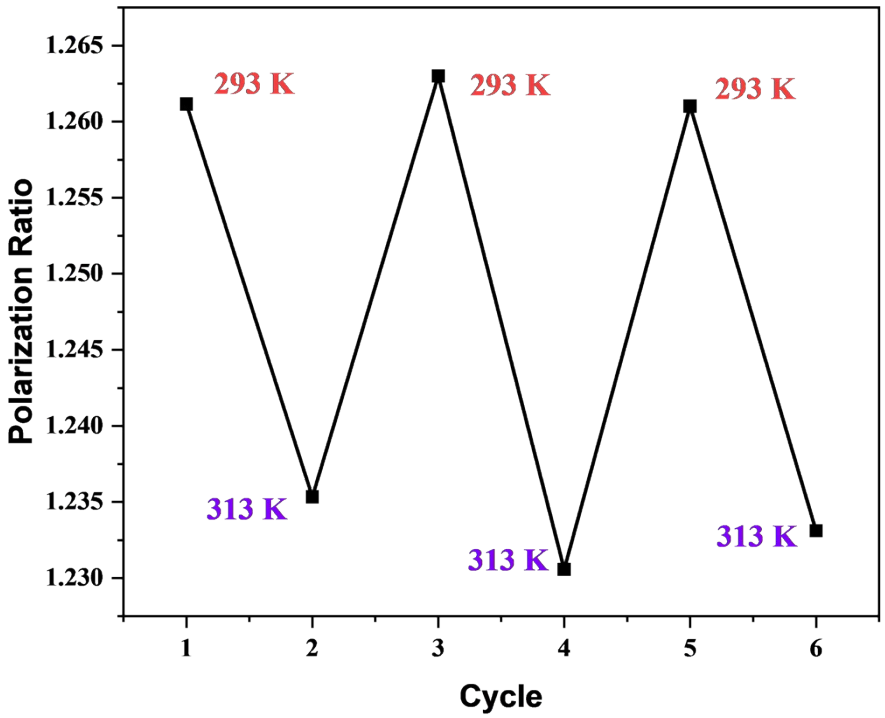

Fig. S18. The relationship between luminescence polarization ratio of **ZJU-28⊃ACF** and temperature during the three thermos-cycles in the range of 293~313 K.